

INTERNATIONAL ATOMIC ENERGY AGENCY  
UNITED NATIONS EDUCATIONAL, SCIENTIFIC AND CULTURAL ORGANIZATION



INTERNATIONAL CENTRE FOR THEORETICAL PHYSICS  
34100 TRIESTE (ITALY) - P.O.B. 586 - MIRAMARE - STRADA COSTIERA 11 - TELEPHONE: 2340-1  
CABLE: CENTRATOM - TELEX 460892-I

H4.SMR/303 - 33

WORKSHOP  
GLOBAL GEOPHYSICAL INFORMATICS WITH APPLICATIONS TO  
RESEARCH IN EARTHQUAKE PREDICTIONS AND REDUCTION OF  
SEISMIC RISK

(15 November - 16 December 1985)

COMPUTER SIMULATION OF FORESHOCK OCCURENCE

B. ANDRE

Centre for Geophysical Research  
Escuela de Física  
Univ. de Costa Rica  
San José, Costa Rica

## Introduction to fractals

The concept of fractals has been on the air for quite some time. Geologists were dealing with it, without knowing it, when they felt forced to include some sort of scale (a ruler, a knife, a person) in the picture of a fracture system in order to give the reader an idea of the size of the system. This idea has been used by several researchers to put forward arguments about the self-similarity of a fracture system. They took a set of photographs, with the help of a microscope, of a small section of a fractured rock, and compared it to sets of photographs of fractures in the soil, and fractures of large regions as they appear when looked from high altitudes. The similarity was striking!

Because of this, I will define in a loose way, a fractal geometry as that which describes the system in which increasing details are revealed by increasing magnification. As the newly revealed structures look similar to those one can see at lower level of magnification, one calls this property SELF-SIMILARITY.

This property is in no way obvious. Quite the opposite, it runs against the notions we learn in regular calculus courses. Just think about the way a simple derivative is defined. The curve near the point of interest is amplified enough to be able to consider it a straight line whose slope equals the value of the derivative at that point. Could this definition be applicable should the curve be a fractal?

To obtain a better information about fractals let us, for the sake of the argument, analyse functions whose value is bounded between -1 and 1 in the whole 1-D space.

One obvious choice, but probably the least common, is the function  $f(x) = \text{constant}$ . Usually this is an uninteresting static case, except for cases like the civil engineer when they better have their buildings designed in such a way that they are static.

Another choice is  $g(x) = \tanh(x)$ , which does vary, but is single valued.

Let us now turn our attention to a multiple valued function  $h(x) = \sin x$ . It is a well known fact that if we chose a point  $x=a$ , the value of  $h(a)$  will be the same for the set  $a+2n\pi$ . For the particular case  $a=0$  there is an extra set of points  $a+(2n+1)\pi$  product of the symmetry  $a \rightarrow -a$ . However if we include the extra information: the sign of the slope at  $a=0$  be the same, the symmetry is broken and we go back to the initial periodic condition.

All through this analysis we have care for the case when the VALUES of a given function remain constant. If we are going to deal with self-similarity, we have to look further, and declare that the "shape" of the function be periodic, as it will be shown below.

Another way of stating the property of self-similarity is stating that there are some physical properties of a given system that will have the same structure

regardless of the length of the scale, i.e. regardless of whether we have contracted or dilated the system.

Mathematically, if  $R$  is a measure of the length of the original state, the property  $P(R)$  will have to be the same for  $R'=aR$ , be  $a<1$  or  $a>1$ .

Hence:

$$P(R') = P(aR) = P(R) A(a) \quad (1)$$

The scale factor  $A(a)$  is included because the actual value of the property may change due to a change of scale. Remember the usual first year Physics course question: If while you are sleeping every dimension of every object in the world around you is reduced to a half, including yourself, will you find out that this has happened? (We are not interested at this moment on the possibility of using material strength, and the like to answer the question, sorry.)

If relation (1) is to be satisfied for any value of  $a$ , the solution is

$$P(R) = R^d \quad A(a) = a^d \quad (2)$$

for any value of the real  $d$ .

It is not uncommon to find examples of fractals which put some constraint on the values  $a$  can take, without losing the property of self-similarity. A very

interesting case is that of  $a=a_0^n$   $n=1,2,3,4,\dots$  for which

$$P(R') = P(a_0^n R) = P(R) A(a_0^n) \quad (3)$$

The standard way to proceed from here consists of looking, based on result (2), for a relationship of the form

$$P(R) = f(R) R^d \quad (4)$$

which when applied on (3) leads to

$$\begin{aligned} P(R') &= P(R) A(a) \\ f(R') R'^d &= f(R) R^d \\ f(a_0^n R) a_0^{nd} R^d &= f(R) R^d A(a_0^n) \end{aligned}$$

The last equality can be split into

$$A(a_0^n) = a_0^{nd} \quad f(a_0^n R) = f(R) \quad (5)$$

Relation (5) could be guessed from (1) and (4) because is an expression of the

fact that the new function  $f$  has to be scale invariant.

Defining a new variable  $y = \ln(R)$  one finds

$$y' = \ln R' = \ln(aR) = n \ln a_0 + \ln R = n \ln a_0 + y$$

and hence

$$g(y') = g(n \ln a_0 + y) = g(y) \quad (6)$$

In summary. When dealing with systems where discrete scaling applies, we can expect a power law modulated by a periodic function in  $\ln R$ , with period  $\ln a_0$ .

**WARNING:** true self-similarity requires more than one fractal dimension.

Now a few remarks on the role of computers when modelling using fractal systems. Usually the computer is used to calculate functions of several variables with utmost precision, or else to expand known theories: many body problems, movement from 1D to 3D, and so forth. When using fractals, however, the computer simulations play the role of a experiment. Even in the case a theory is found, one would have a subset of the necessary information, but not the whole structure. This is caused by the fact that the system shows deterministic chaotic behavior. Thus the solutions will diverge exponentially as the experiment progresses, even though the initial conditions are almost the same. This statement ceases to be true if we have attractors. In that case the solutions will look very similar, regardless of the initial conditions, i.e. we have a pattern. One may say one has reached dynamical equilibrium, as in the case of a gas at constant volume and pressure.

#### MODEL OF EARTHQUAKE DYNAMICS

What follows is a brief description of the model developed by Dr. L. Knopoff, Dr. T. Yamashita and myself at the Institute of Geophysics and Planetary Physics, of Univ. of California.

Let us start by postulating that earthquakes show a fractal behavior. Taking advantage of the hierarchy subjacent in this concept, we developed only one of the levels, making it valid for the other levels based on the self-similarity property.

Work by L. Knopoff and Y. Kagan shows that if earthquakes are treated as points, the distribution of the distance  $x$  between any two points will follow within reasonable limits (the maximum distance for which this applies is of the order of a plate, some 2000 Km) the relation  $1/x^\alpha$ .

Should one use the area  $A$  covered by any three points, the distribution is  $1/A^\beta$ . In

the case one works with the volume  $V$  limited by 4 non-planar points the

applicable relation looks like  $1/V^\gamma$ .

But earthquakes are not points, but fractures or cracks. We will choose the crack size in our model using the distribution based on  $1/x^\alpha$ , where  $x$  is now between an upper and a lower limit. The actual size is chosen from a random flat distribution between to given limits.

Thus far the only crack distribution that has been solved exactly in an analytical manner is that of a line of cracks of equal size ( $r$ ) equally spaced by a distance  $s$ . In principle, an expression well known to students, any crack configuration can be solved using the techniques developed by Mushkelishvili, using complex variable formalism.

Chatterjee, Mal and Knopoff succeeded in solving the case of two parallel non-linear cracks with a good accuracy, by solving a system of two coupled integro-differential equations. A comparison of the solution one obtains using the analytical result and that derived by Chatterjee is shown in Figure 1. The role stress corrosion plays in our model is explained further down.

Because of this difficulty one is bound to simulate the fractured region as a set of parallel line of cracks, as shown in figure 2.

Every crack is taken to interact with any other in a pair-wise way, that is to say, the two cracks will be considered to be embedded in a perfect elastic media with no other crack present.

Even in this simplified model, we are bound to have lots of difficulties. In Figure 3 I present the calculated and experimental stress patterns for a crack under three different conditions. The complexity of the patterns makes it impossible to write a program which will calculate the corresponding pattern for each crack, at each step of the program. Hence the only solution available was to consider that all the stress is concentrated at the tips (no relation with the M8 algorithm) varying as the inverse of the square of the distance.

Another problem that had to be solved was the mode of fracture that was to be used. This was not that difficult, because here again we have not very many possibilities open. Out of the three fundamental modes of fracture it is found that Mode I fracture cannot happen at the Earth's interior, for it represents a tensile fracture, as shown in Figure 4. Mode III, in the other hand is the mode to be used should one want to apply the model to subduction zones. Its tensorial nature, however, makes it impossible to use in our model. Hence we are left with Mode II. Lest I give the impression that this choice is a simple one, I include the solution obtained for the seismic moment of two collinear parallel cracks, whose tips are at  $x=a, x=b$  and  $x=c, x=d$ . The solution includes elliptical integrals, a fact in favor of using computers for our simulation.

To get the system moving we have to include time. For that we referred to literature and settle for the fact that cracks grow under the influence of stress corrosion. Figure 5 is taken from an article by Atkinson, who has published extensively on the subject. It can be seen that the velocity of growth is related to a parameter  $K$  known as stress intensity factor, a concept familiar to those involved in material sciences. It has been found that when this factor reaches a

given critical value  $K_C$ , the crack grows in a self-sustained manner at a sizable speed.

In our model the value of  $K$  is calculated in a for each crack at every step of the program. Because its actual value depends on the stress field applied to the crack, and this in turn is a function of the crack distribution, this is one of the most time consuming parts of the program. The time that has to be dedicated to this task grows almost exponentially with the number of cracks and lines involved. This is one of the factors that make this type of programs not amenable to be solved with a personal computer. At the rate the personal computers are growing, it is not at all silly to think that in the near future this situation will be reversed.

The concept of  $K_C$  is included in our model in the following manner. The space between two contiguous collinear cracks is assigned a particular value of  $K_C$ , chosen from a flat random distribution. This particular choice is prompted by the lack of experimental data.

Having set the scenario, let the actors play their role.

The script is as follows. A time step is calculated and the cracks are let to grow with the velocity  $v = b K^{20}$ . The exponent 20 was chosen out of a set of values determined experimentally, whose upper value may be as high as 65!!.

The choice of this rule is caused by the fact that we will like to modelled the behavior of a initially fractured zone when enough time has elapsed to take to the region marked 3 in Figure 5.

After all the cracks are allowed to grow, the stress field is recalculated, and new values of  $K$  are also calculated. This a time consuming part of the program.

Should the recalculated values of  $K$  be in any instance larger than the associated value of  $K_C$ , the contiguous cracks are taken to fuse immediately, given rise to a small event. The fact that we take the speed of fusion to be infinite is a figure of speech based on the evidence that even in the worst case, events of magnitude 9, the time invested in ruptures of several kilometers is at most a couple of minutes, a very small time indeed with respect to that necessary to prepare that event.

Because of the possibility of a run away situation in which a crack may grow and grown, the program stops time and recalculate again the stress and the  $K$  of all the cracks. It then checks for any other situation in which  $K$  can be larger than the associated  $K_C$ . If that is the case another fusion happens. This process is repeated as many times as necessary. One can claim then, that the event is being simulated by a multiple source mechanism.

In the event no further fusion is permitted, time is increased and the overall process is repeated.

## RESULTS 1

Some of the results that can be presented for this type of approach are shown in Figure 6. The time  $T=0$  corresponds to the main shock, which in this context corresponds to that event with the maximum seismic moment. Each bar represents the number of events that occur  $n$  units of time before the main shock. A very

important point in this graph is the fact that regardless of the time unit used, the three curves look the same. This is what is to be expected from self-similarity in time, a property NOT explicitly included in the model, but expected from the analysis Y. Kagan did with some thousands of real events. Any seismologist will recognize any of this curves as a graphic representation of Omori's law of foreshocks. How well this compares with reality can be seen by comparison with Figure 7.

## Scene 2: TECTONICS

Thus far we have played with stress re-distribution, time delays (i.e. stress corrosion), and fractals. A new actor is required: Plate Tectonics.

The inclusion of such a phenomena was not as easy as may be thought. A first, and immediate step, was to take the external stress to increase as a function of time. We think anyone will agree with our choice: a linear relationship. After some testing, however, it became clear that the lowest value of stress should be approximated to zero. In other words, we should work with the stress drop of the event, for which we have values available. This was fortunate, for otherwise we would have to find values for the stress in the "relaxed" state: that is, the stress present in the region after the big event has happen and the aftershocks had occurred. By big event we have in mind magnitude 8 and above. An even harder problem was to find the rate the stress build up in time due only to tectonics. Our solution was to scale the time using as unit the time it took to have the the whole process happen when tectonics was turn off, and the whole process was driven totally by stress corrosion. Niceties of modelling!

An adjustable parameter was initially included, but soon forgotten when we found out it was not necessary. In this way we were able to handle the tectonic effect without any adjustable parameter, without sacrificing self-similarity.

## Scene 3: ASPERITIES

The concept of asperities is now current currency among seismologist. It explains in a simple manner different observed phenomena. It can be applied to subduction and transform faults, may be used to explain aftershocks and doughnut patterns, or the different seismicity of different regions, Figures 8 and 9. Its inception in our model can be done in several alternate ways. One could claim that the biggest spaces between the cracks in a given line could be associated to asperities, given them no special treatment when assigning the values of  $K_C$ . One can also work backwards: choosing several spaces at random, and assigning them a value of  $K_C$  higher than the maximum used for the rest. A third and last alternative, is to single out a few of the biggest spaces and assigning them higher values of  $K_C$ . We adopted the last one.

The results shown here were obtained as follows: an initial run is done with tectonics turn off, in order to find the scaling time, and identify the location of

the asperities. Extra runs are then carried out with tectonics, using the same initial parameters, and keeping the asperities in exactly the same place and state as during the initial run. The only change is the crack distribution between the asperities. The rationale is that the asperities correspond to places where geometry, and may be other material properties, act in such a way that any change will be of transient nature.

## RESULTS 2

Among the several results we have obtained thus far with our model, I can mention:

a) The ratio of the time the main shock occurs relative to the time the initial happens, varies from  $10^3$  to  $10^7$ , depending on crack distribution. Such a ratio is consistently 2 to 3 when tectonics is present.

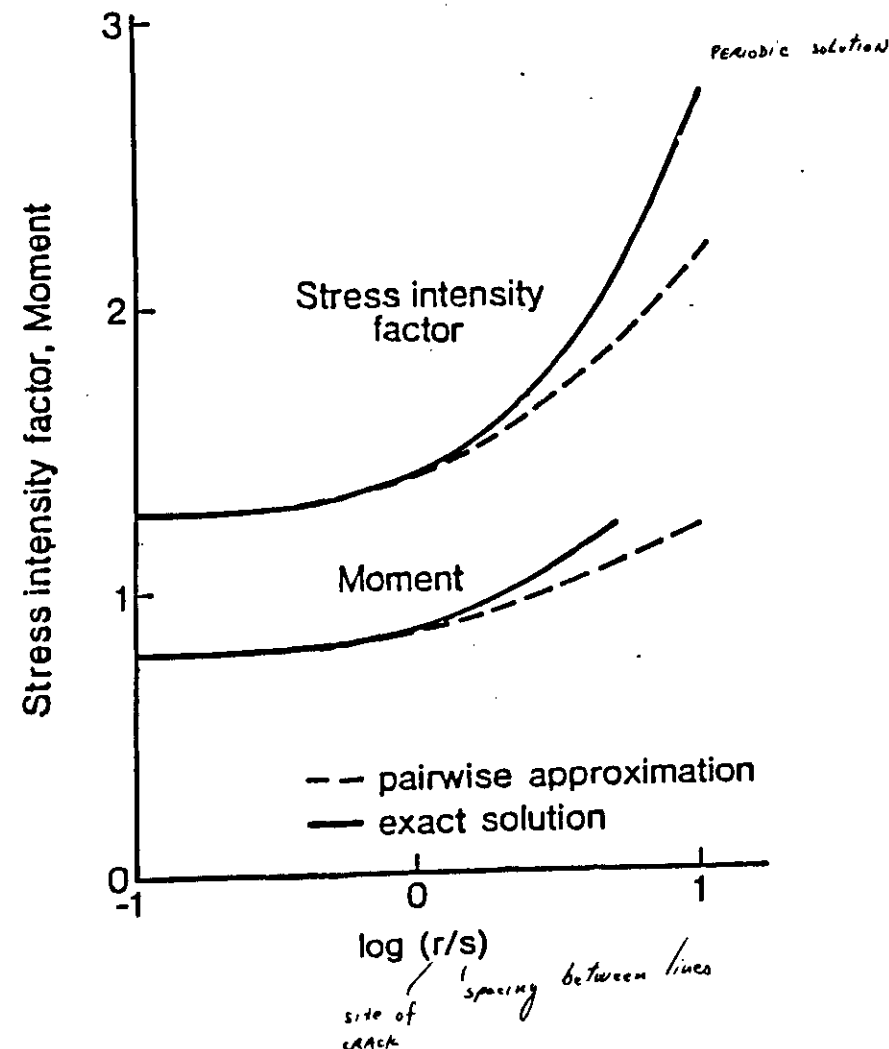
In order to be able to compare different runs, a catalog is prepared by normalizing time and magnitude with the values relative to the main shock. By main shock we understand that which has the highest seismic moment, not necessarily the last one.

b) For the geometry 80 cracks and 1 line, we found that even if the  $K_C$  associated with asperities is 3 times the maximum used, several aftershocks occur, without involving any of the asperities. Also, the rupture of an asperity is not necessarily associated with the main shock. This is particularly valid for cases when two asperities are present and they are located toward one end of the line.

c) For a geometry of 20 cracks and 4 lines, foreshocks and aftershocks are commonly present. Figure 10 and 11 show the result of two runs with the same initial conditions except that the  $K_C$  is 2, and 3 times the maximum. One notices that the strong shock before the main one, happens at about the same time, not so with the other events.

d) The foreshock pattern is quite random, as can be seen by comparing Figures 11 and 12.

e) An initial test for a relationship of the actual time of the main shock with the respective magnitude is now in progress.



Asperity.

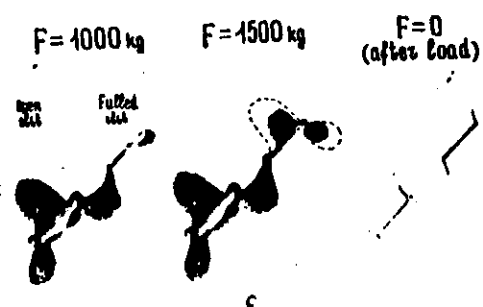
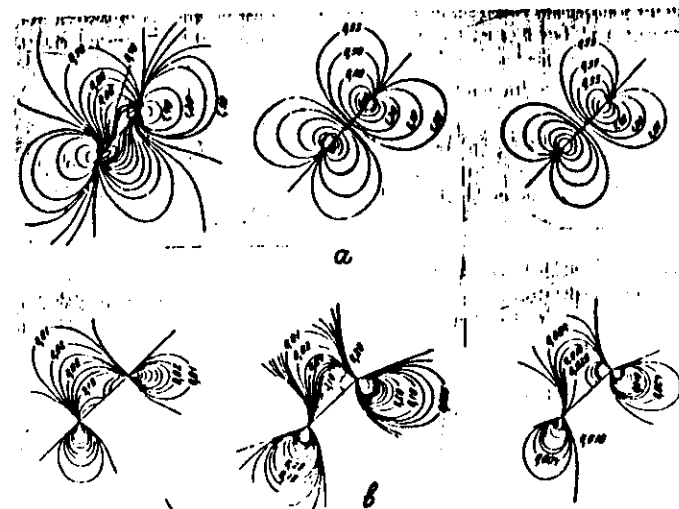
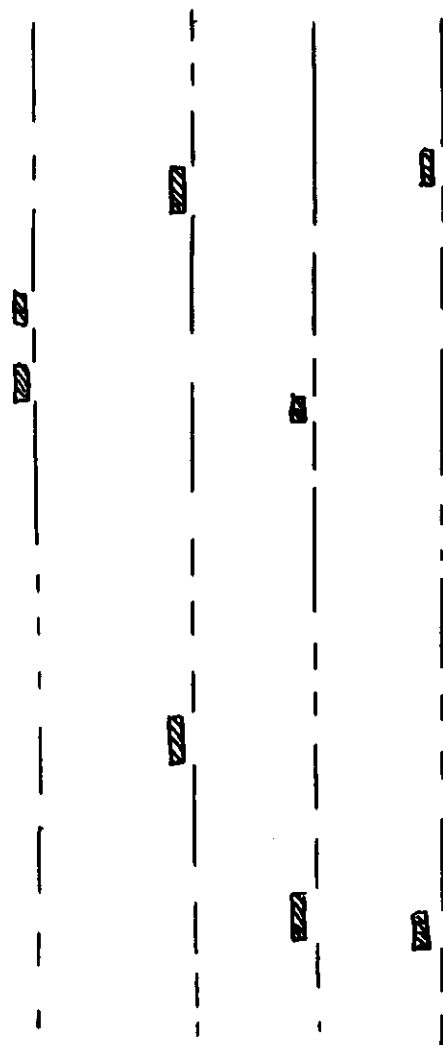


Figure 1  
(a)  $\sigma_{xx}$ , and (b)  $\text{grad } \sigma_{xx}$  contour lines; on the left, open fracture; in the middle, closed fracture without friction; on the right, perfectly rigid inclusion. Dashed region correspond to  $\sigma_{xx} < 0$  (quantitative estimation  $\sigma_{xx} < 0$  was not made). (c) Schlieren photo of the specimen. Compression everywhere is vertical.

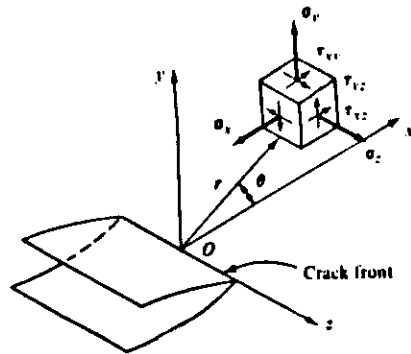


Figure 3-5

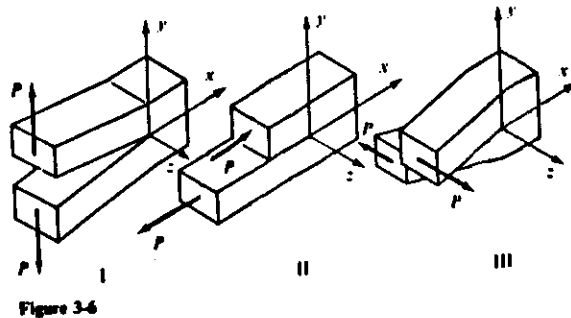


Figure 3-6

$$\begin{aligned}
 H/\sigma_0(1-\nu) &= 2 \int_d^c (s^2 + C_1 s + C_2) \left( \frac{c-s}{(s-d)(b-s)(a-s)} \right)^{\frac{1}{2}} ds \\
 &= ((a-c)/(b-d))^{\frac{1}{2}} ((b-c)(a+b-c-d)K(k) \\
 &\quad + (b-d)(3c-a-b-d)E(k))/2 + \pi((a+b-c-d)^2 - 4(a-c)(b-d) \\
 &\quad E(k)/K(k))(1-\Lambda_0(\theta, k))/4 \\
 \Lambda_0(\theta, k) &= 2(E(k)F(\theta, k') + K(k)E(\theta, k') - K(k)F(\theta, k'))/\pi, \\
 (k')^2 &= 1 - k^2, \quad \theta = \sin^{-1}((1-\delta^2)^{\frac{1}{2}}/k') \quad \delta^2 = (c-d)/(b-d)
 \end{aligned}$$

$F(\theta, k')$  and  $E(\theta, k')$  are incomplete elliptic integrals of the first and second kinds.

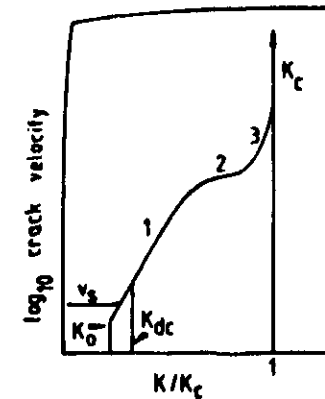


Fig. 20. Schematic diagram showing the influence of stress intensity factor on subcritical crack growth behavior in a rock undergoing stress corrosion.  $K_c$  and regions 1, 2, and 3 of stress corrosion behavior are as for Figure 1.  $K_0$  is the stress corrosion crack growth limit,  $v_0$  is the crack velocity threshold due purely to dissolution at the crack tip, and  $K_{dc}$  is the crack growth limit below which bulk diffusion creep dominates deformation behavior.  $K_{dc}$  may be located at stress intensities above or below  $K_0$ , depending on the temperature. Its location in this figure is chosen for convenience of representation. Note normalized stress intensity factor axis. Temperature, pressure, and activity of stress corrosion agent are all held constant.

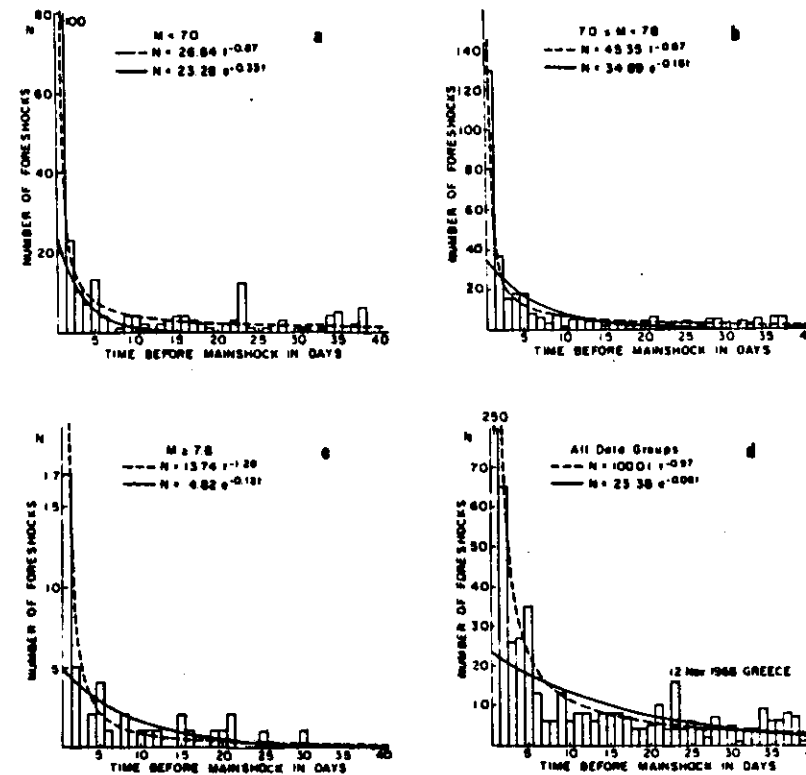
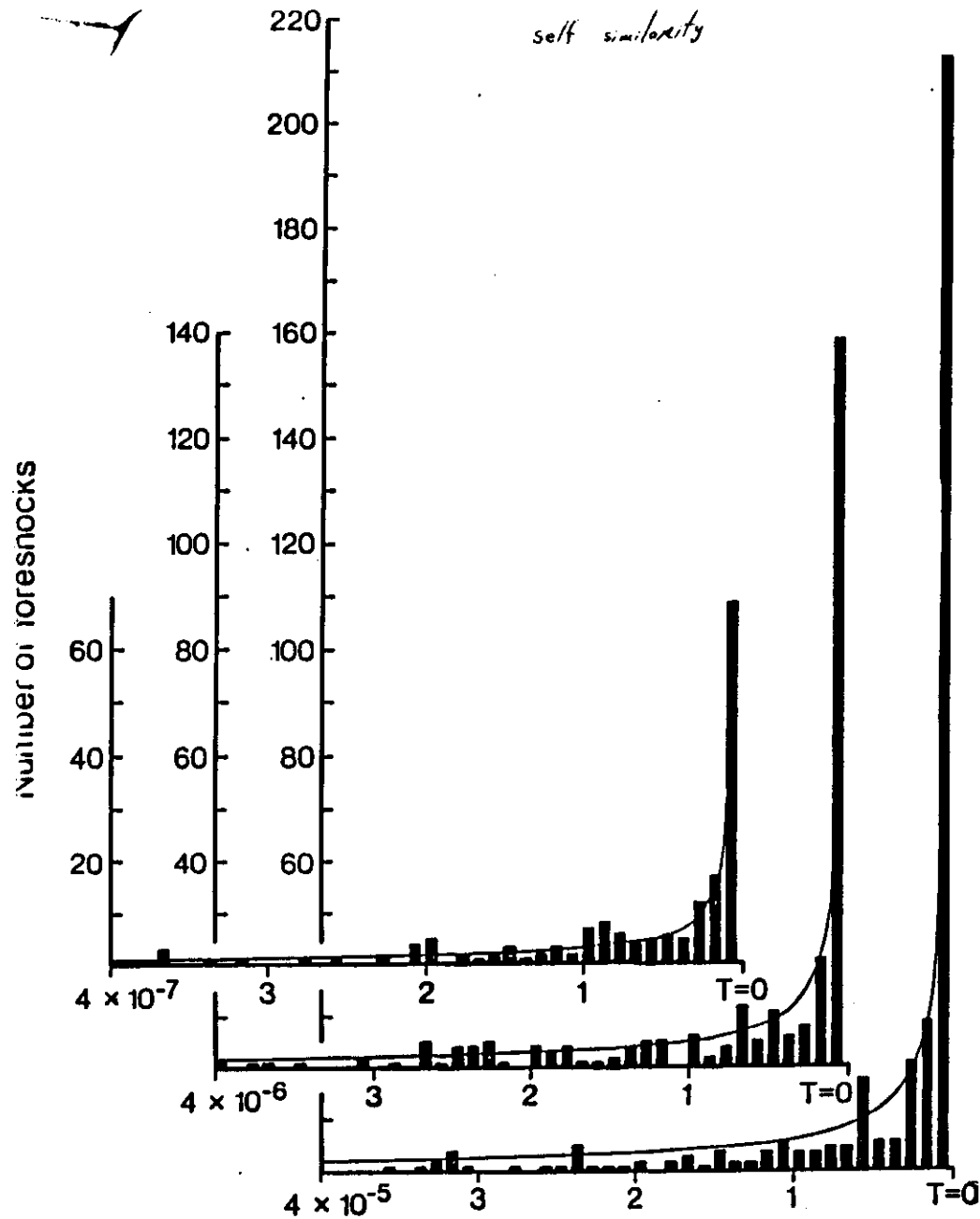
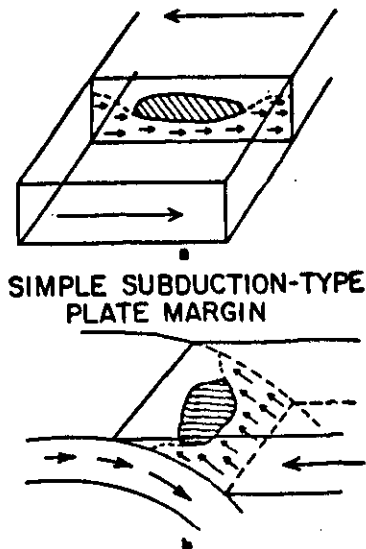


Fig. 7. Foreshock activity (a-c) as a function of time before main shocks of different magnitudes and (d) for all main shocks from all three data sets. Also shown are the exponential (solid line) and power law (dotted line) equations that best fit these data. Note that the temporal variation does not depend upon the magnitude of the main shock.





**SIMPLE SUBDUCTION-TYPE  
PLATE MARGIN**

Fig. 1. Progression of a slipping front across a plate margin of (a) transform type, and (b) subduction type.

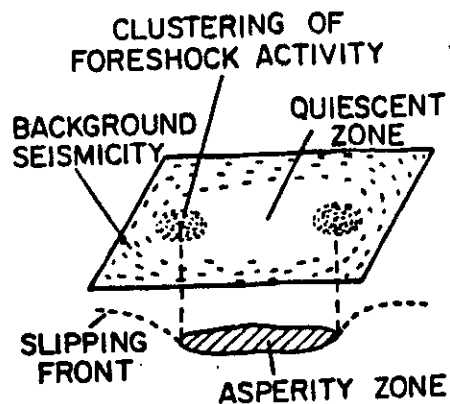


Fig. 2. Seismicity pattern created by progression of a slipping front across a plate margin with an asperity.

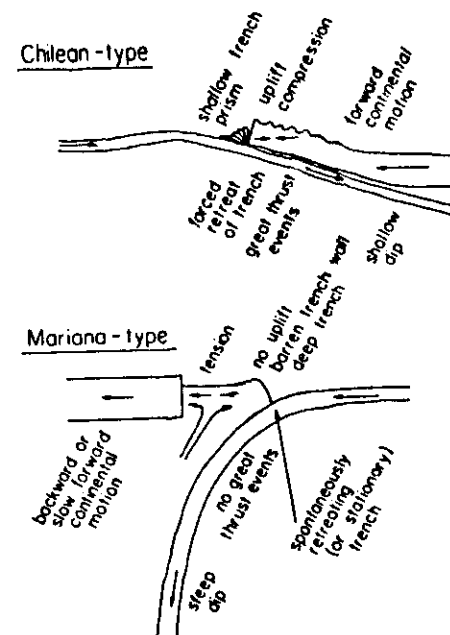


Fig. 3. Diagrams showing characteristics of strongly coupled (Chilean type) and weakly coupled (Mariana type) subduction zones (modified from Uyeda and Kanamori, 1979).

